INSTITUTE OF TECHNOLOGY

AIR UNIVERSITY

UNITED STATES AIR FORCE

SCHOOL OF ENGINEERING

THESIS

WRIGHT-PATTERSON AIR FORCE BASE, OHIO

AF-WP-8-SEP 60 5M

SYNTHESIS OF AMPLIFIER CIRCUITS USING MORE THAN ONE TUNNEL DIODE

THESIS

Presented to the Faculty of the School of Engineering
The Institute of Technology
Air University
in Partial Fulfillment of the
Requirements for the
Master of Science Degree
in Electrical Engineering

By
Richard R. Wong, B.S.E.E.
Capt USAF
Graduate Electrical Engineering
August 1961

Preface

This report is the result of my attempt to produce some concrete evidence that an amplifier circuit containing more than one tunnel diode can be built. It is written with the assumption that the readers are familiar with modern network synthesis techniques and their limitations because the method used in the report is based on the synthesis of passive networks. The method, predistortion, is applied in reverse to synthesize an experimental circuit containing two tunnel diodes.

In the experimental results section, no data below 1000 cps is available because of the erratic operation of the circuit. After the circuit was constructed and in operation, I spent most of my time trying to determine the cause of this erratic operation; however, I was unsuccessful. The second attempt at finding the solution was also unsuccessful because of the lack of proper components and the lack of time. Other than this omission, I believe that this report proves the value of the predistortion procedure as applied to tunnel diodes.

Since I was not familiar with either the tunnel diode or the synthesis of passive network, I had to do a large amount of research and reading on both subject. To list the many articles and books that were read would only add bulk; therefore, the bibliography contains only those articles and books which are referred to in the body and the Appendices.

I wish to express my gratitude to Major Everette T. Garrett, Mr. Carl K. Greene, and Mr. Dan Enxing for the time that they have so willingly spent in consultations.

Richard R. Wong

Contents

Abstract

The predistortion procedure is used to synthesize a two tunnel-diode amplifier. This amplifier is evaluated and compared with the theoretical gain and bandwidth calculated from the transfer function of forward voltage gain that was used to synthesize the circuit. Problems that made the experimental circuit bandwidth smaller than the theoretical bandwidth were the poor isolation between the bias circuit and the ac signal circuit and the effects of parasitic or stray capacitances at the high frequency end of the response curves. However, the gain of the amplifier compared favorably with the theoretical maximum gain.

GE/EE/61-16

SYNTHESIS OF AMPLIFIER CIRCUITS USING MORE THAN ONE TUNNEL DIODE

I. Introduction

The purpose of this report is to present a synthesis procedure (Ref 13:66-75) for designing multistage tunnel-diode amplifiers and to present a realizable amplifier designed by this procedure. Discussions in the literature have mentioned some of the difficulties that arise in the design of multistage amplifiers such as how to achieve isolation between stages and how to make tunnel-diode amplifiers unilateral. These difficulties are caused by the two-terminal-bilateral properties of the tunnel diode. In the synthesis procedure presented here, these difficulties are no real problem.

The synthesis procedure is based on the procedure used for designing filter networks and other passive networks. In the synthesizing of passive networks, ideal inductance and capacitance elements are assumed, but when the networks are actually constructed with the physical counterparts of these ideal elements, parasitic elements invariably appear. These parasitic elements have the effect of shifting the location of the poles and zeros of the driving-point or transfer function for which the network was synthesized. The greatest effect is the shifting of the poles and zeros to

the left in the complex s-plane because of the unavoidable dissipation in the reactive elements. As a solution to this problem, predistortion transformation permits parasitic losses to be taken into account in such a way that the desired function is realized exactly (Ref 1:414). This technique provides a series resistance with every inductance of the network and a shunt conductance with every capacitance, but it does not change the shape of the magnitude plot or the phase plot of the prescribed transfer function.

This report presents a detailed discussion of the predistortion technique as applied to passive network synthesis and its adaptation for synthesizing active networks containing tunnel diodes. This procedure, known as reverse predistortion when applied to active networks, is then applied to a low-pass response function to synthesize an amplifier circuit containing two tunnel diodes. Finally, an experimental evaluation of this amplifier in terms of gain, bandwidth, and circuit complexity is given.

II. The Tunnel Diode

General

The Esaki or tunnel diode is a semiconductor p-n junction with an extremely thin barrier or space-charge layer formed between two heavily-doped regions (Ref 8:217). This combination of thin barrier and heavy doping results in the tunnelling effect where particles obeying the laws of quantum theory penetrate the potential barrier even though they do not have sufficient energy to go over the barrier (Ref 5:3). In the tunnel diode, the tunnelling of electrons results in a negative-resistance characteristic in the forward-biased region as shown in Fig. 1. This negative resistance (r_n) is

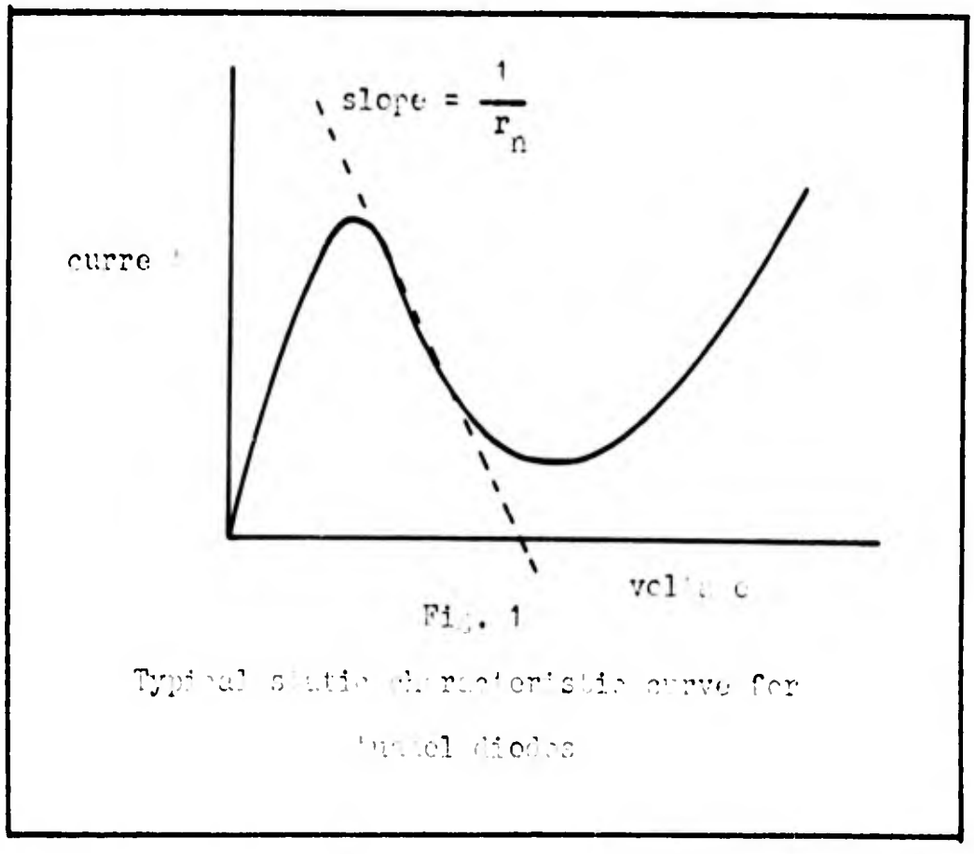

Fig. 1

Typical static characteristic curve for tunnel diodes

the most useful property of the tunnel diode; therefore, why it appears is explained in greater detail.

Principle of Operation

Essentially the tunnel diode is a p-n junction formed with a degenerate n-type semiconductor (Appendix A) and a degenerate p-type semiconductor (Ref 10:1202). When the junction is formed and zero voltage or zero bias is applied, the resulting tunnel-diode characteristic in terms of the simple band picture is Fig. 2(a) where the electrons are at the same level on both sides of the junction and no net current flows. If a small forward bias is applied, some of the electrons at the bottom of the conduction band in the n-side are now opposite empty states of the valence band of the p-side of the junction. Forward current flows and increases with bias until a maximum is reached as in Fig. 2(b). At the maximum-current point further increase in forward bias brings the forbidden region of the p-side opposite the conduction electrons on the n-side and fewer and fewer electrons are able to see empty states to which they can tunnel; therefore, the current decreases as in Fig. 2(c). Finally, with further increase in bias, minority carrier injection takes place giving rise to the normal forward characteristic of a p-n junction diode to complete the tunnel diode characteristic of Fig. 2(d)

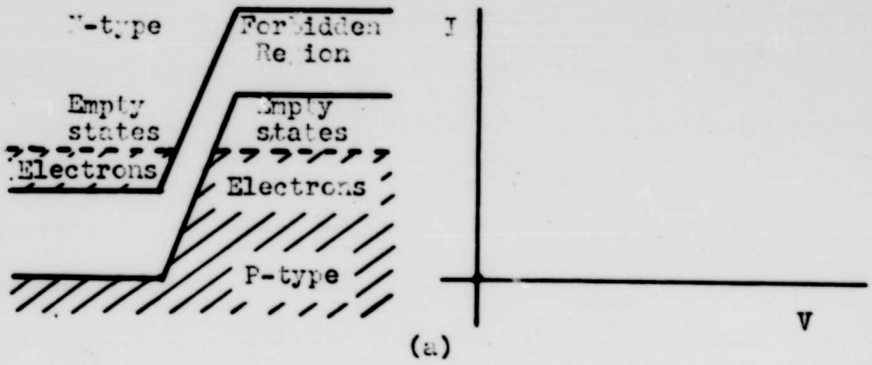

(a)

Electrons are at the same level on both sides of the junction. No net current flows.

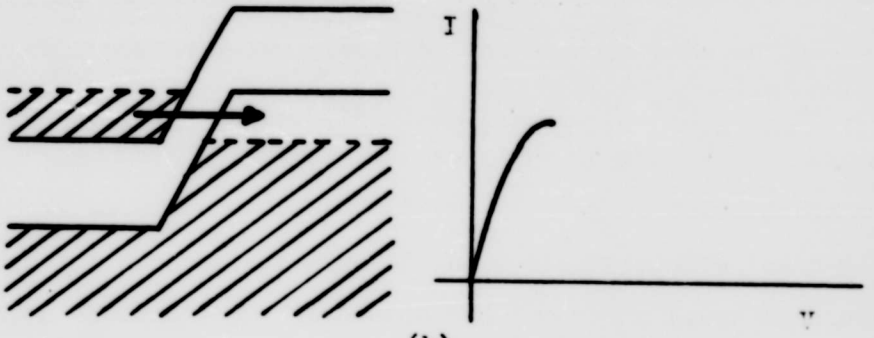

(b)

Electrons on the left are raised until they are opposite empty states on the right. Current flows from left to right and increases to a maximum.

Fig. 2

Tunnel diode characteristics in terms of the simple band pictures

Parts (a) and (b)

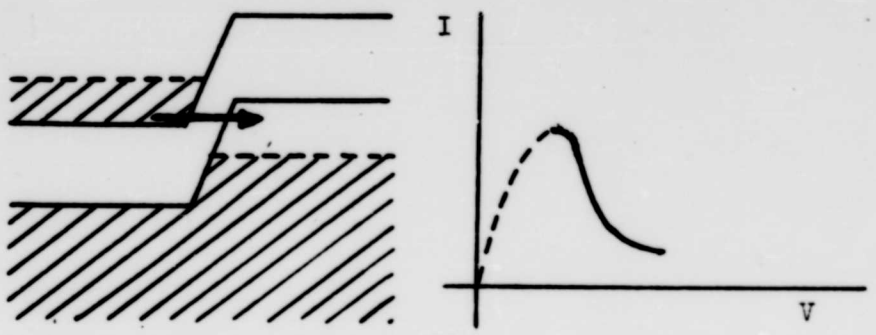

(c)

Some of the electrons on the left are opposite empty states on the right. Current decreases.

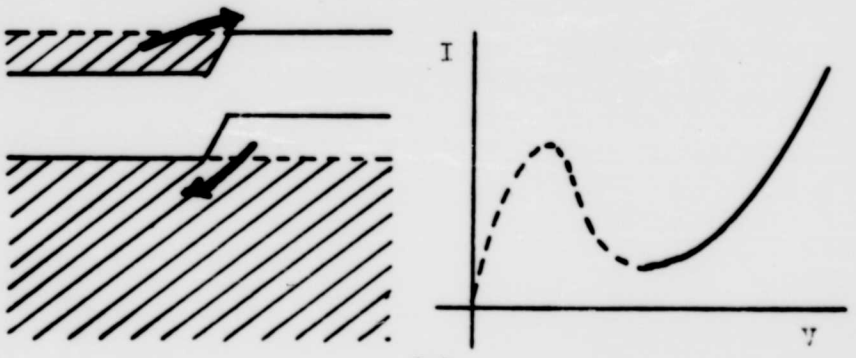

(d)

Electrons are raised until carrier injection takes place over the barrier.

Current increases.

Fig. 2

Tunnel diode characteristics in terms of the simple band pictures

Parts (c) and (d)

Equivalent Circuit

In the negative-resistance region, the equivalent circuit of the tunnel diode consists of a negative resistance (r_n) shunted by a capacitance (C) in series with a positive resistance (R_s) and an inductance (L_s) as shown in Fig. 3.

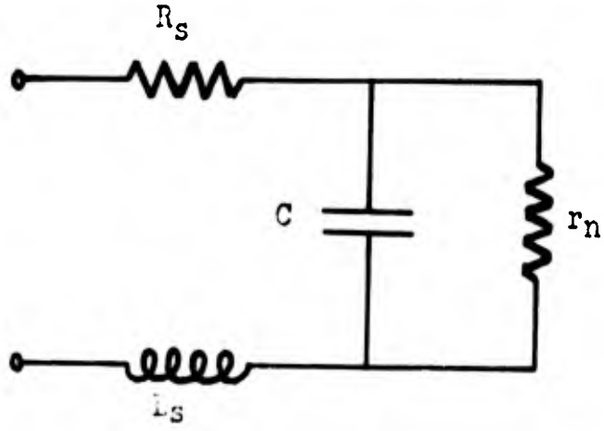

Fig. 3

Equivalent circuit of the tunnel diode in the negative resistance region

The negative resistance is practically independent of frequency from dc to beyond the microwave region, and it can be made substantially independent of temperature (Ref 5:6). The other three parameters (R_s, L_s, C) are the limiting factors in the frequency performance of the tunnel diode.

Capacity C is primarily due to the capacity of the junction although a small portion is contributed by the leads and the packaging. Series inductance L_s results from the leads, and series resistance R_s is a combination of lead resistance and bulk resistance of the semiconductor material.

Another element that might be included in the tunnel diode equivalent circuit is a noise generator in parallel with r_n because the tunnel diode exhibits shot noise in the negative-resistance region. The mean square noise current from the noise generator is given by the formula (Ref 2:37)

$$\overline{i_n^2} = 2eI \Delta F \qquad (1)$$

where e = electronic charge

I = average current (dc)

ΔF = observation bandwidth

This noise generator is represented by a generator labeled $\overline{i_n^2}$ in parallel with r_n, but it is usually not included in the equivalent circuit.

Frequency Limitation

The four elements as shown in the equivalent circuit determine the resistive cutoff frequency (f_{ro}) and the reactive cutoff frequency (f_{xo}) of the tunnel diode (Ref 3:14). The resistive cutoff frequency is the maximum frequency the tunnel diode can amplify. It is the frequency at which the real part of the diode impedance measured at its terminals goes to zero. This frequency, f_{ro}, can be calculated by

$$f_{ro} = \frac{1}{2\pi C|r_n|}\left[\frac{|r_n|}{R_s} - 1\right]^{\frac{1}{2}} \qquad (2)$$

(Appendix B)

The reactive cutoff frequency is the frequency at which the reactive part of the diode impedance goes to zero. This is the frequency at which the inductance and capacitance will resonate if the device were ac short-circuited (Ref 4:110). This frequency, f_{xo}, can be calculated by

$$f_{xo} = \frac{1}{2\pi}\left[\frac{1}{L_s C} - \frac{1}{r_n^2 C^2}\right]^{\frac{1}{2}} \qquad (3)$$

(Appendix B)

Although f_{ro} and f_{xo} are limiting cases for the tunnel diode package, both frequencies are highly circuit dependent.

Stability

The first consideration in using a tunnel diode for amplification is stability. To obtain a stable dc operating point in the negative-resistance region, the internal resistance of the biasing source (R_b) must be chosen such that the dc load line intersects the diode characteristic at only one point as shown in Fig. 4. Consequently, the biasing source must have a resistance that is less than the absolute value of the negative resistance or

$$R_b < |r_n| \qquad (4)$$

This is the dc stability criterion (Ref 8:220). Maintaining the dc operating point is a big problem in the design of tunnel diode amplifiers. Since the negative resistance is not linear, slight variations in bias resulting in a change of negative resistance can cause large changes in

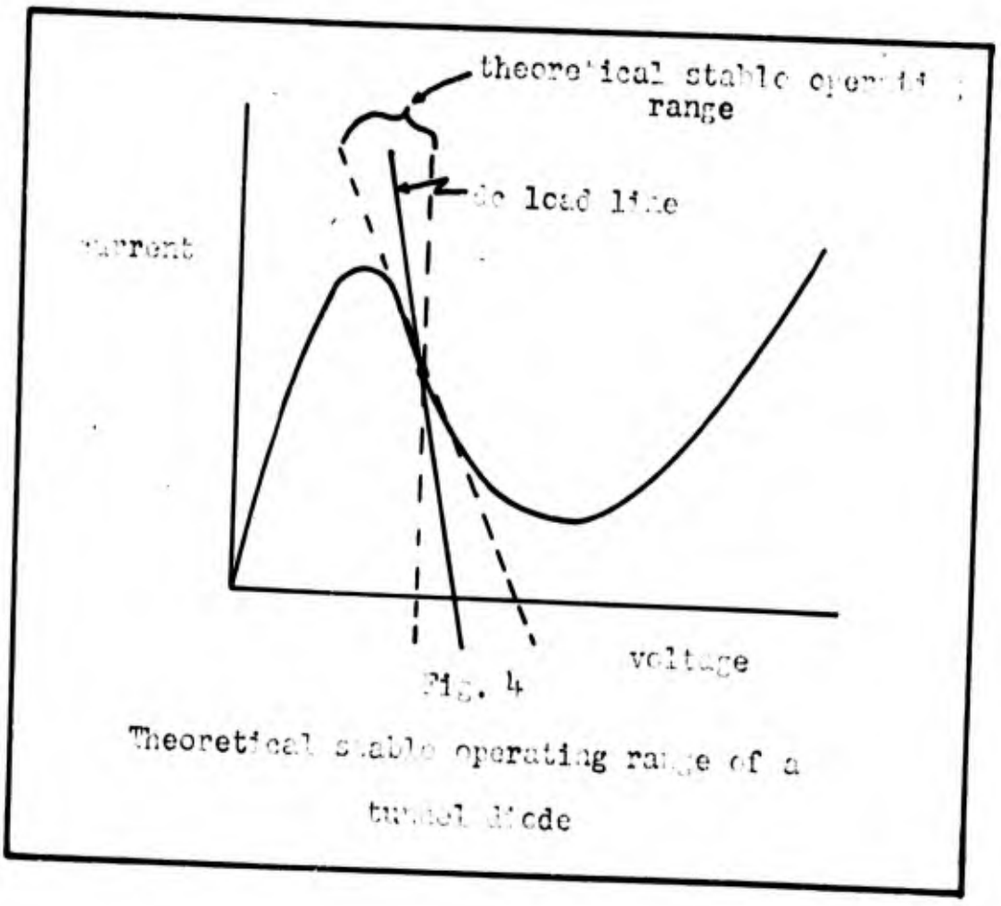

Fig. 4

Theoretical stable operating range of a tunnel diode

gain. Therefore, a very stable bias supply is a necessity for stable amplifier operation.

Another stability criterion that must be satisfied for amplification is the dynamic or ac stability given by

$$R_T > \frac{L_T}{C\,|r_n|} \tag{5}$$

where R_T = total incremental resistance

L_T = total circuit inductance

C = total diode capacitance

r_n = negative resistance of the tunnel diode

This equation, Eq 5, is obtained from the distribution of

poles and zeros of the circuit input impedance in the complex s-plane. If the zeros of the imput impedance fall in the left half side of the s-plane, the circuit is stable. If they fall in the right half plane the circuit is unstable (Ref 3:22).

The stability criterion, the bilateral properties, and the inherent low power output has limited the application of the tunnel diode. The reverse predistortion synthesis method may be a partial solution to these problems. Since the predistortion method moves the poles and zeros of a transfer function further to the left of the imaginary axis, the system should become more stable. Also in predistortion synthesis the bilateral properties of the tunnel diode present no problem because the method is based on the use of precisely such networks. Finally, the possibility of using more than one tunnel diode in an amplifier circuit should increase the circuit power output.

III. Predistortion

Applied to Passive Networks

The predistortion technique suggested by Weinberg (Ref 13:66-75) is based on the synthesis of lossless passive networks. In the practical realization of a lossless network, resistance is unavoidable because of the inductor resistance or capacitor leakage. The presence of this resistance distorts the transfer function of the actual network realization in comparison with the lossless design.

Consider the LC network with these resistances added as shown in Fig. 5. Added for each L or C element is a resistance or conductance such that the ratio of R/L or G/C

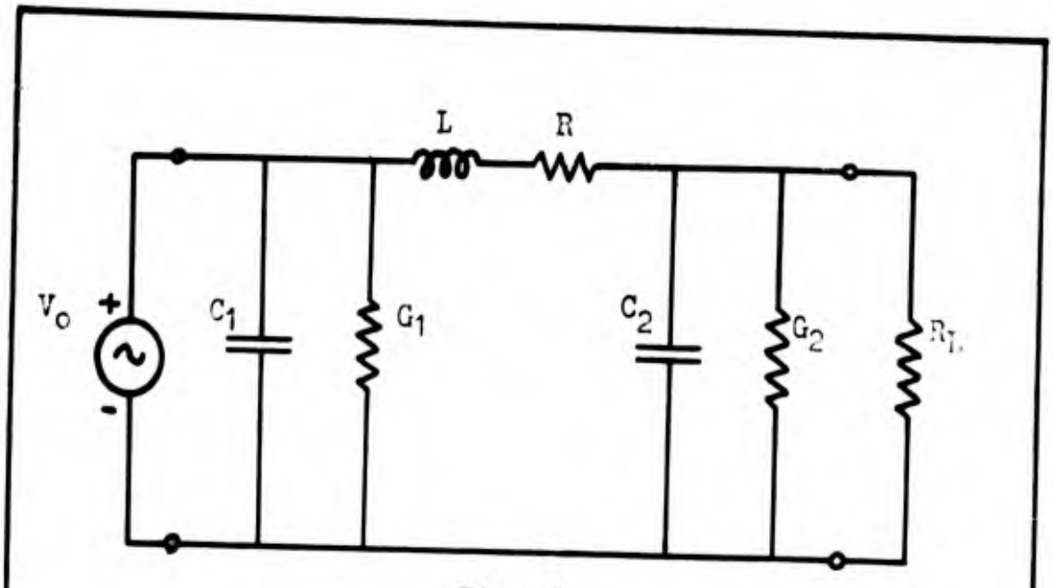

Fig. 5

LC circuit with inductor resistance and capacitor leakage

is equal to the same constant d. The impedance of an original inductance becomes the impedance of a series RL branch.

$$sL \rightarrow sL + R = L(s + d) \tag{6}$$

The admittance of the original capacitance becomes the admittance of a shunt GC branch.

$$sC_1 \rightarrow sC_1 + G_1 = C_1(s + d) \tag{7}$$

and

$$sC_2 \rightarrow sC_2 + G_2 = C_2(s + d) \tag{8}$$

Thus, the original forward transfer impedance $Z_{21}(s)$ becomes $Z_{21}(s + d)$ with the addition of the resistances. In terms of the poles, the resistances have the effect of translating the real frequency axis ($j\omega$ axis) by the amount d to the right as shown in Fig. 6.

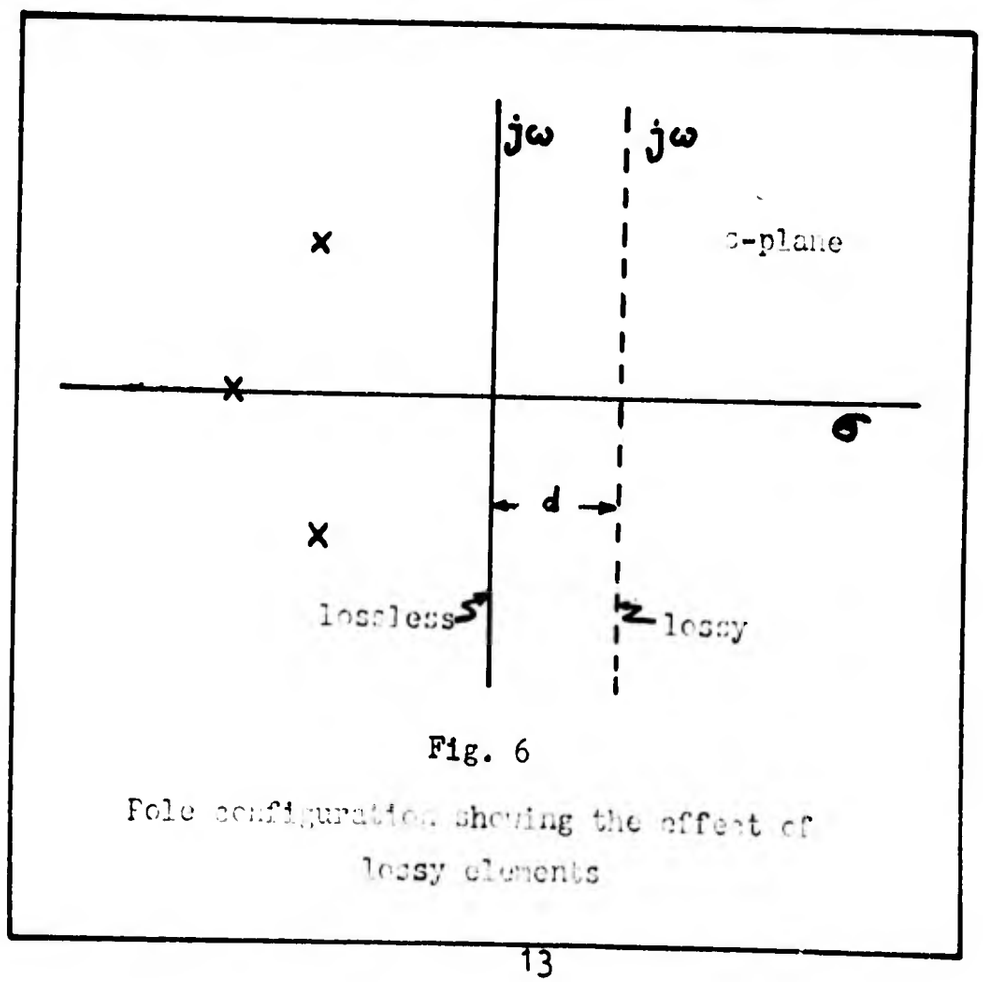

Fig. 6

Pole configuration showing the effect of lossy elements

In the uniform predistortion technique, the real frequency axis is shifted to the left by the amount d causing the desired $Z_{21}(s)$ to become $Z_{21}(s - d)$. This technique provides a series resistance with every inductance of the network and a shunt conductance with every capacitance without changing the magnitude or the phase of the prescribed transfer function when the network is synthesized using $Z_{21}(s - d)$. In the actual construction of the network, the losses of the inductances and the capacitances are adjusted by addition of appropriate resistances to achieve the desired pole-zero configuration (Ref 6:114-116). In this process of uniform predistortion and then removal, the only change in the transfer function is the constant multiplier. It is decreased causing a flat loss to be introduced.

Applied to Active Networks

For the realization of an active network, the predistortion technique is used in reverse. The real frequency axis is translated by an amount d to the right. As a result, the original transfer function to be synthesized is transformed to a function of s + d. The transformed transfer function is synthesized by conventional methods as in passive networks. Then the predistortion is removed by shunting a negative conductance of amount $C_n d$ across each capacitor C_n and placing a negative resistance of amount $L_n d$ in series with each inductance L_n (Ref 13:67).

If this reverse predistortion (Ref 13:67) is carried out properly, the final network, which requires negative resistances for realization, yields voltage and power gain unobtainable with passive networks. Consider the case of a transfer function

$$G(s) = K \frac{\prod_{i=1}^{m} (s + a_i)}{\prod_{j=1}^{n} (s + b_j)} \tag{9}$$

which is assumed to be realizable using R and C elements only. In such a circuit the maximum value of the multiplier, K_{max}, that can be realized is given by

$$K_{max} = \frac{\prod_{1}^{n} b_j}{\prod_{1}^{m} a_i} \tag{10}$$

When the real frequency axis is translated by an amount d to the right, the transformed transfer function G'(s) is given by

$$G'(s) = K' \frac{\prod_{i=1}^{m} (s + a_i + d)}{\prod_{j=1}^{n} (s + b_j + d)} \tag{11}$$

The maximum value of K'_{max} that can be realized when G'(s) is synthesized is

$$K'_{max} = \frac{\prod_{j=1}^{n} (b_j + d)}{\prod_{i=1}^{m} (a_i + d)} \tag{12}$$

which can be greater than K_{max}. Upon removal of the predistortion by shunting a negative conductance of amount $C_n d$ across each capacitor the transfer function becomes

$$G''(s) = K' \frac{\prod_{i=1}^{m} (s + a_i)}{\prod_{j=1}^{n} (s + b_j)} \qquad (13)$$

Thus, with K' as the new multiplier, a flat gain has been introduced by the addition and removal of the predistortion.

Since the poles and zeros of the original transfer function are not changed by the addition and removal of predistortion, the shape of the magnitude plot and phase plot remains the same. However, the final transfer function, Eq 13, is displaced upward because of the increase in the constant multiplier.

In realizing G"(s) of Eq 13, any of the varied techniques of passive network synthesis may be used depending upon the requirements or specifications given. For a system function of an RC network, LC network, or RLC network, the limits of the predistortion procedure depends upon the realizability conditions on the various types of system functions. The restrictions on the realizability of the passive networks also restrict active network realization. These restrictions are too numerous to list, but they may be found in any book on modern network synthesis.

From the stability viewpoint, the method of realizing the final network and the restrictions placed on the system

function guarantee the stability of the complete network. In the reverse predistortion technique the poles and zeros of the original function and the final transfer function remain the same; consequently, if the original transfer function is stable, the final transfer function is stable.

An Active Network Example

As an example of the reverse predistortion procedure, suppose it is desired to synthesize a transfer function $G_{12}(s)$ given by

$$G_{12}(s) = K \frac{1}{(s + 1/2)(s + 3/2)} \qquad (14)$$

which represents a low pass RC network (Ref 12:437) with all its poles lying on the negative real axis. The maximum value of $K_{max} = 3/4$ when $\omega = 0$. If an amount of predistortion $d = 1/2$ is added, the real frequency axis is translated 1/2 unit to the right. This can be seen in Fig. 7 which shows the pole-zero configuration before and after predistortion.

The distorted transfer function $G'_{12}(s)$ is

$$G'_{12}(s) = K' \frac{1}{(s + 1)(s + 2)} \qquad (15)$$

At $\omega = 0$ the maximum value of the constant multiplier is $K'_{max} = 2$. When the predistortion is removed the final transfer function $G''_{12}(s)$ is

$$G''_{12}(s) = \frac{2}{(s + 1/2)(s + 3/2)} \qquad (16)$$

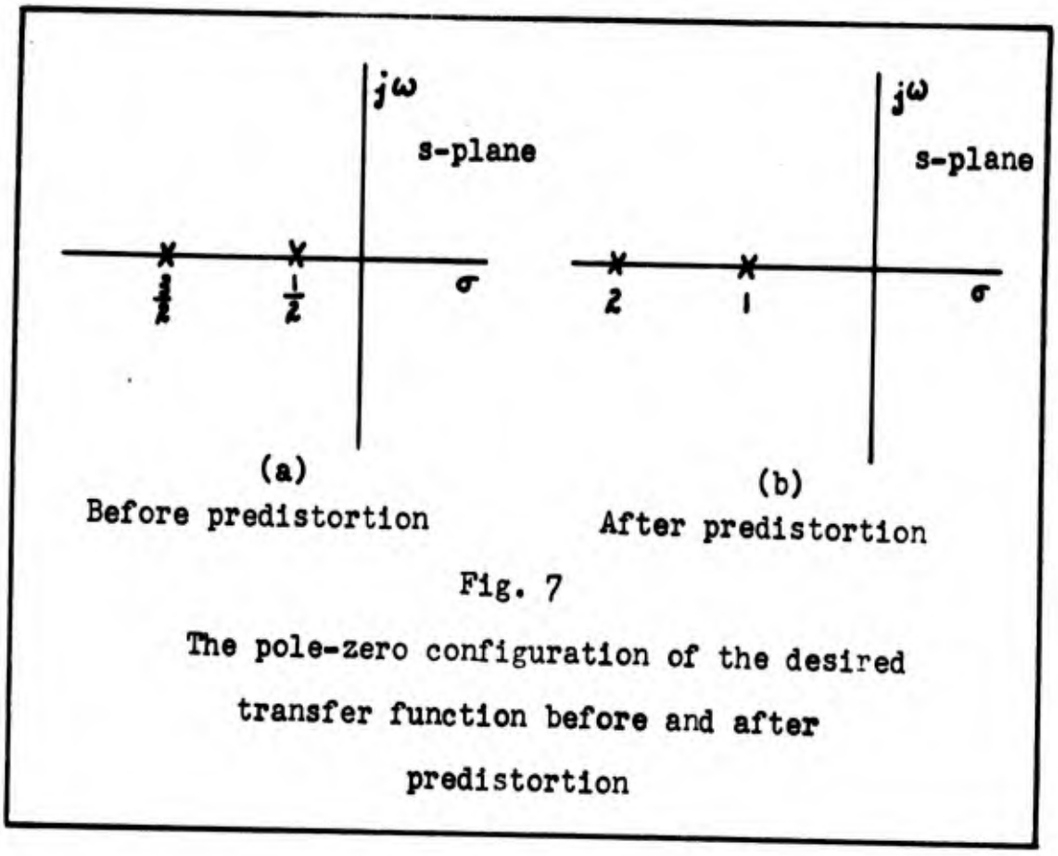

Fig. 7

The pole-zero configuration of the desired transfer function before and after predistortion

As a result of the addition and removal of the predistortion, the constant multiplier of the original transfer function Eq 14 has been increased.

Since the only change from the original transfer function is the increase in magnitude of the multiplier, the magnitude plot should have the same shape. Again referring to the example, the plots of the original transfer function Eq 14 and the final transfer function after a cycle of predistortion addition and removal, Eq 16, are shown in Fig. 8. It can be seen that the shapes are exactly the same except for the increase in magnitude of the final transfer

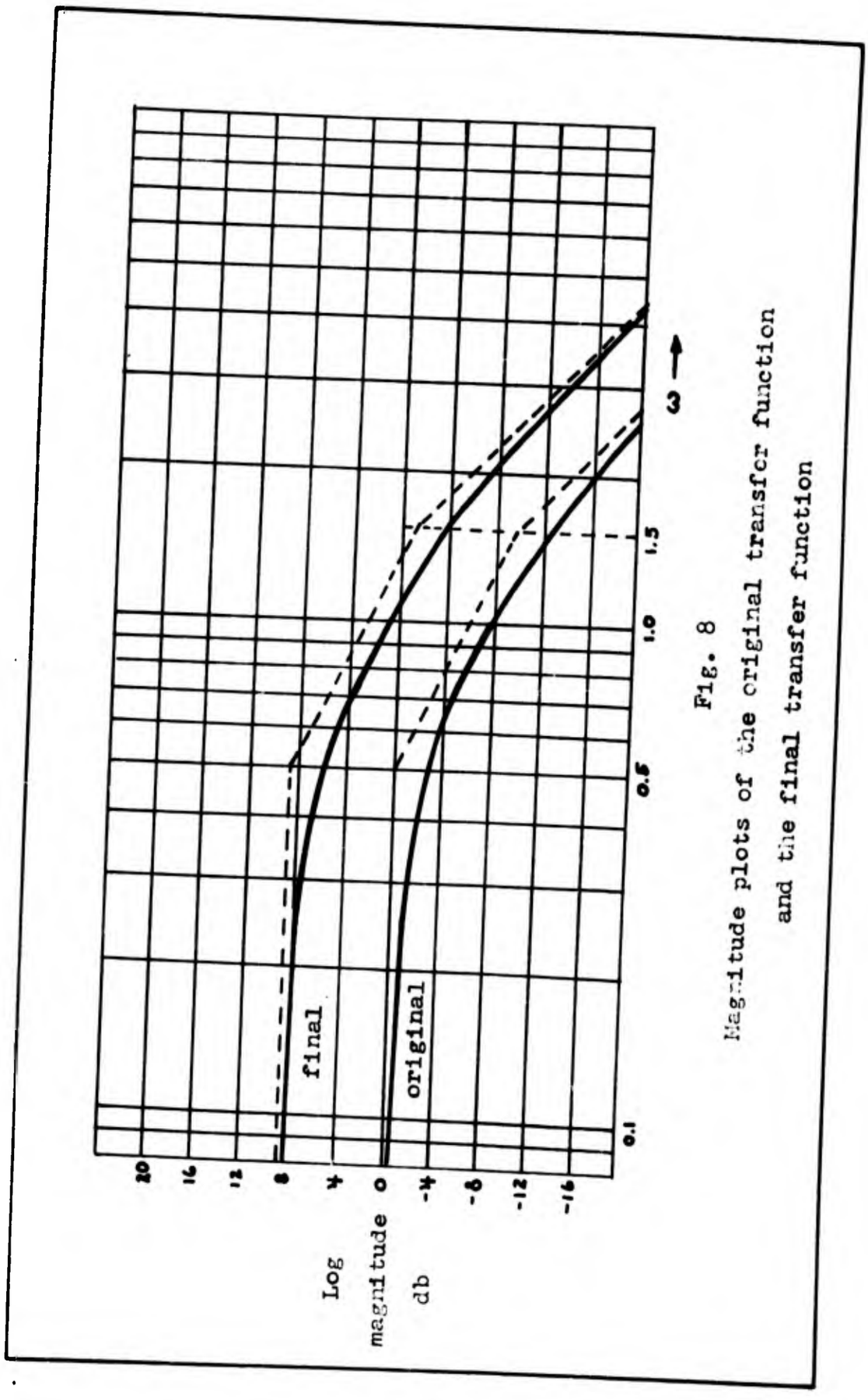

Fig. 8
Magnitude plots of the original transfer function and the final transfer function

function. Since the shape of the magnitude plot has not changed, the shape of the phase plot also remains unchanged.

Although the example used is an RC network, the method of reverse predistortion is general. It can be applied to any type of system function as long as the restrictions to that particular type are not violated. Its use can introduce a voltage gain as well as a power gain into the system, essentially making an amplifier out of a passive network. An amplifier synthesized by this method is experimentally evaluated in the next section.

IV. Synthesis of an Amplifier Using the Predistortion Technique

Synthesis of the Normalized Amplifier

The predistortion technique discussed in section III is now applied to designing an amplifier containing two tunnel diodes. Assume that the amplifier desired is to have the same magnitude plots shown in Fig. 8. The desired transfer function is then given by

$$G_{12}(s) = \frac{E_{out}}{E_{in}} = K \frac{1}{(s + 1/2)(s + 3/2)} \qquad (17)$$

Other specifications are the source resistance must equal the load resistance and the gain must be optimized to the highest value when the amount of predistortion d = 1/2. The specifications are all normalized values.

Adding the predistortion d = 1/2 to the transfer function of Eq 17, the resulting predistorted function is

$$G'_{12}(s) = K' \frac{1}{(s + 1)(s + 2)} \qquad (18)$$

which is the function for which the network is synthesized. Because of the specifications given, the method that is used was devised by E.S. Kuh (Ref 12:437-444) where the gain constant is optimized to the highest value. Applying the Kuh method to the transfer function of Eq 18 results in the normalized network of Fig. 9 where all the values are given in ohms and farads.

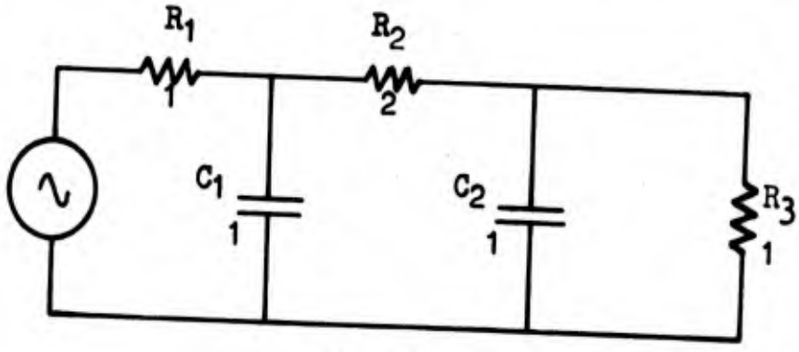

Fig. 9

Predistorted normalized network synthesized from $G_{12}'(s) = K' \frac{1}{(s+1)(s+2)}$

To remove the predistortion, a negative resistance of an amount

$$r_n = - \frac{1}{C\ d} \tag{19}$$

is shunted across each capacitance. Therefore,

$$r_{n1} = - \frac{1}{(1/2)(1)} = -2 \text{ ohms} \tag{20}$$

and

$$r_{n2} = - \frac{1}{(1/2)(1)} = -2 \text{ ohms} \tag{21}$$

Then the normalized network becomes the network shown in Fig. 10.

Experimental Circuit

In the denormalized network each resistance is multiplied by the magnitude factor (R_o) and each capacitor is divided by the product of the magnitude factor and the frequency factor ($2\pi f_o$) (Ref 9:50).

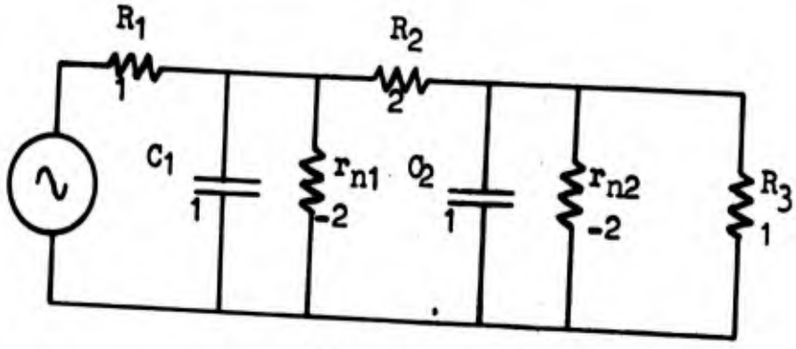

Fig. 10

Normalized network with the predistortion removed

For the experimental circuit $R_o = 50$ is used to calculate the values of the elements given in Table I. In this same table, there are three values of f_o which indicate the frequencies for which evaluation of the circuit is made.

Table I

Values Used in the Experimental Circuit

$R_o = 50$ for all calculations

Case	f_o (Kcps)	ω_o (rad/sec)	C_1 & C_2 (μfd)	R_1 & R_3 (ohms)	R_2 (ohms)	r_{n1} & r_{n2} (ohms)
A	57.9	0.363M	0.055	50	100	-100
B	91.0	0.571M	0.035	50	100	-100
C	212.0	1.330M	0.015	50	100	-100

The final circuit that is experimentally evaluated is shown in Fig. 11.

In this circuit, the negative resistances are replaced by 1N2939 tunnel diodes with the following measured values

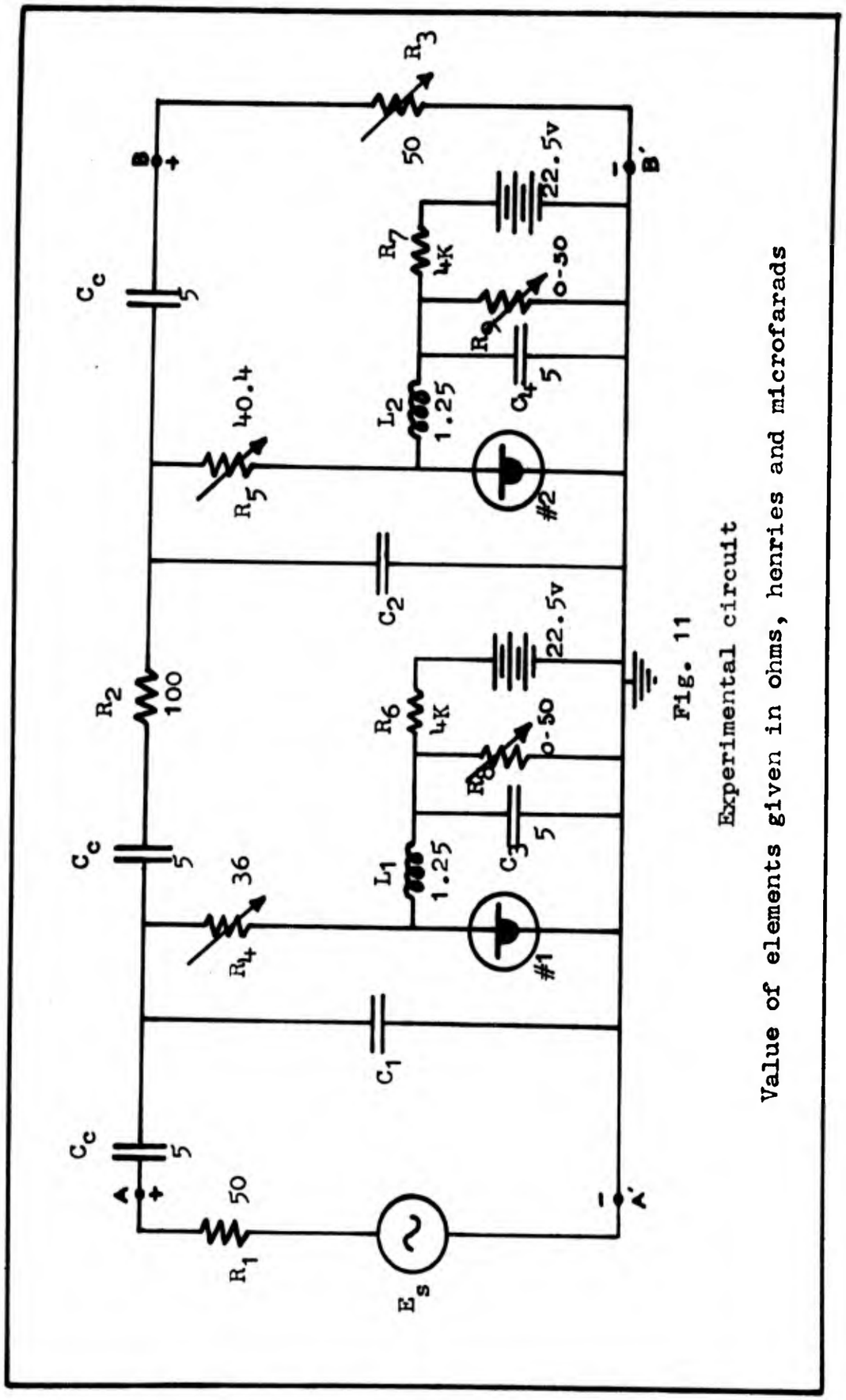

Fig. 11

Experimental circuit

Value of elements given in ohms, henries and microfarads

of negative resistance and junction capacitance and specified values of series inductance and series resistance (Ref 3:87).

Tunnel Diode #1 $r'_{n1} = -137.5$ ohms at the Q-point
$I_{o1} = 0.6$ ma
$V_{o1} = 100$ mv
$C = 10.6 \mu\mu f$
$L_s = 6$ mμh
$R_s = 1.5$ ohms

Tunnel Diode #2 $r'_{n2} = -141.9$ ohms at the Q-point
$I_{o2} = 0.6$ ma
$V_{o2} = 120$ mv
$C = 14.6 \mu\mu f$
$L_s = 6$ mμh
$R_s = 1.5$ ohms

Since the negative resistance desired in each shunt branch is only -100 ohms, a positive resistance $R_4 = 36$ ohms and $R_5 = 40.4$ ohms is necessary in each branch as shown. Therefore, in branch #1

$$r_{n1} = -137.5 + 1.5 + 36 = -100 \text{ ohms} \quad (22)$$

and in branch #2

$$r_{n2} = -141.9 + 1.5 + 40.4 = -100 \text{ ohms} \quad (23)$$

Bias Circuit

To maintain the Q-point for each of the tunnel diodes, the circuit of Fig. 12 is used. In this circuit, two 2.5 henry chokes in parallel to lower the dc resistance to 43.3 ohms for L_1 and 40.0 ohms for L_2 and a bypass capacitor

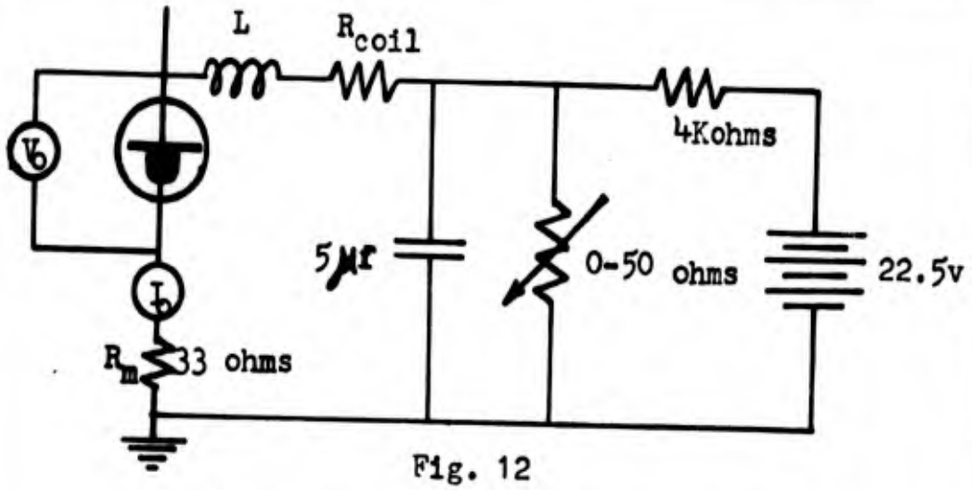

Fig. 12

Bias circuit for the experimental circuit

of 5 microfarads are used to isolate the dc power supply from the ac signal. The dc power supply is a 22.5 volt battery with a voltage divider network of 4000 ohms and a 0-50 ohm variable resistor which is varied to obtain and maintain the Q-point in the negative-resistance region at I_{o1} = 0.6 ma and V_{o1} = 100 mv for diode #1 and I_{o2} = 0.6 ma and V_{o2} = 120 mv for diode #2. With this arrangement, the dc resistance of the biasing circuit (R_b) will satisfy the dc stability criterion of Eq 4 since

$$R_{b1} < |r'_{n1}| \tag{24}$$

and

$$R_{b2} < |r'_{n2}| \tag{25}$$

With the biasing circuit included, the final experimental circuit is as shown in Fig. 11. In this circuit,

there are three coupling capacitors (C_c), each equal to 5 microfarads, that are necessary to separate the dc biasing circuit from the rest of the circuit. Otherwise, the circuit is similar to the normalized circuit of Fig. 10 where R_1 represents the source resistance and R_3 represents the load resistance assuming purely resistive terminations.

Theoretical Gain and Bandwidth

Since the circuit is synthesized from the transfer function of Eq 18 which is

$$G'_{12}(s) = K' \frac{1}{(s + 1)(s + 2)} \tag{26}$$

$K'_{max} = 2$ at zero frequency. After the predistortion is removed, the final circuit represents the function

$$G''_{12}(s) = \frac{2}{(s + 1/2)(s + 3/2)} \tag{27}$$

When Eq 27 is expressed in corner plot form, it becomes

$$G''_{12}(j\omega) = \frac{8/3}{\left(1 + j\frac{\omega}{0.5}\right)\left(1 + j\frac{\omega}{1.5}\right)} \tag{28}$$

or

$$G''_{12}(f) = \frac{2.67}{\left(1 + j\frac{f}{0.5f_o}\right)\left(1 + j\frac{f}{1.5f_o}\right)} \tag{29}$$

Therefore, the theoretical maximum gain is 2.67 or 8.54 db at f = 0 cps. The gain decreases continuously as the frequency increases, the amount of decrease being dependent upon the location of the two corner frequencies. The theoretical

bandwidth is from 0 cps to the frequency where the gain has decreased to 5.54 db as shown in Figs. 13, 14, and 15.

From Table I there are three cases to be considered.

Case A: $f_{oA} = 57.9$ Kcps

$$f_{cA1} = (0.5)(57.9K) = 28.95 \text{ Kcps} \quad (30)$$

$$f_{cA2} = (1.5)(57.9K) = 86.9 \text{ Kcps} \quad (31)$$

$$\text{Bandwidth A} = 26.0 \text{ Kcps} \quad (32)$$

Case B: $f_{oB} = 91.0$ Kcps

$$f_{cB1} = (0.5)(91.0K) = 45.5 \text{ Kcps} \quad (33)$$

$$f_{cB2} = (1.5)(91.0K) = 136.5 \text{ Kcps} \quad (34)$$

$$\text{Bandwidth B} = 39.0 \text{ Kcps} \quad (35)$$

Case C: $f_{oC} = 212.0$ Kcps

$$f_{cC1} = (0.5)(212.0K) = 106.0 \text{ Kcps} \quad (36)$$

$$f_{cC2} = (1.5)(212.0K) = 318.0 \text{ Kcps} \quad (37)$$

$$\text{Bandwidth C} = 94.0 \text{ Kcps} \quad (38)$$

Experimental Results

The final circuit of Fig. 11 is constructed as small as possible to minimize the effects of lead inductances and stray capacitances. A calibrated double-beam oscilloscope is used to measure the input ac signal (E_{in}) and the output ac signal (E_{out}), and it also compares the shape of these two signals. One channel of the oscilloscope is connected across terminals AA' and the other channel is connected across terminals BB' of Fig. 11. These two pairs of terminals are the E_{in} and E_{out} terminals respectively. Data for the curves of Figs. 13, 14, and 15 (Appendix D) is taken using the values for the components as given in Table I for each of the three

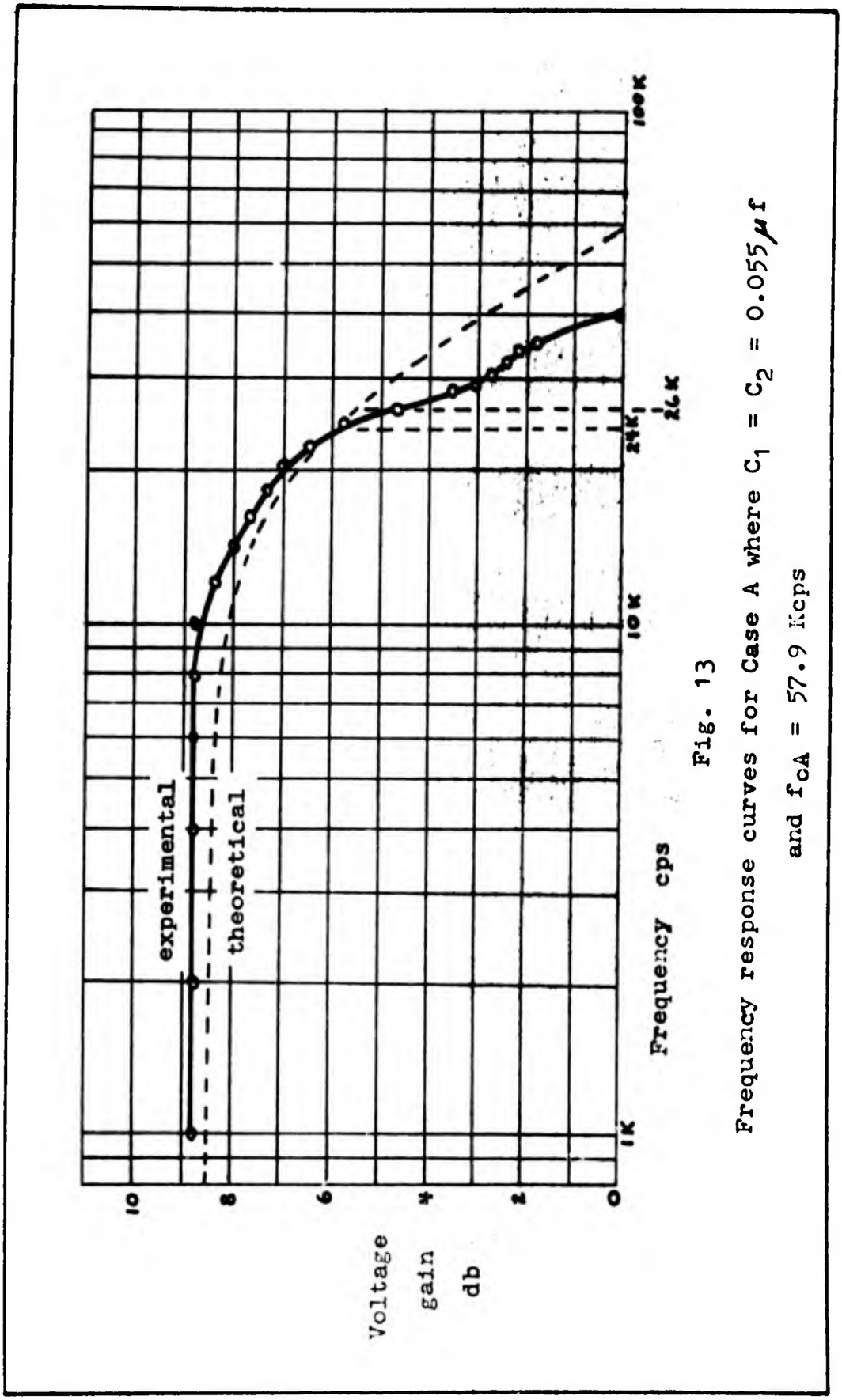

Fig. 13

Frequency response curves for Case A where $C_1 = C_2 = 0.055\mu f$ and $f_{cA} = 57.9$ Kcps

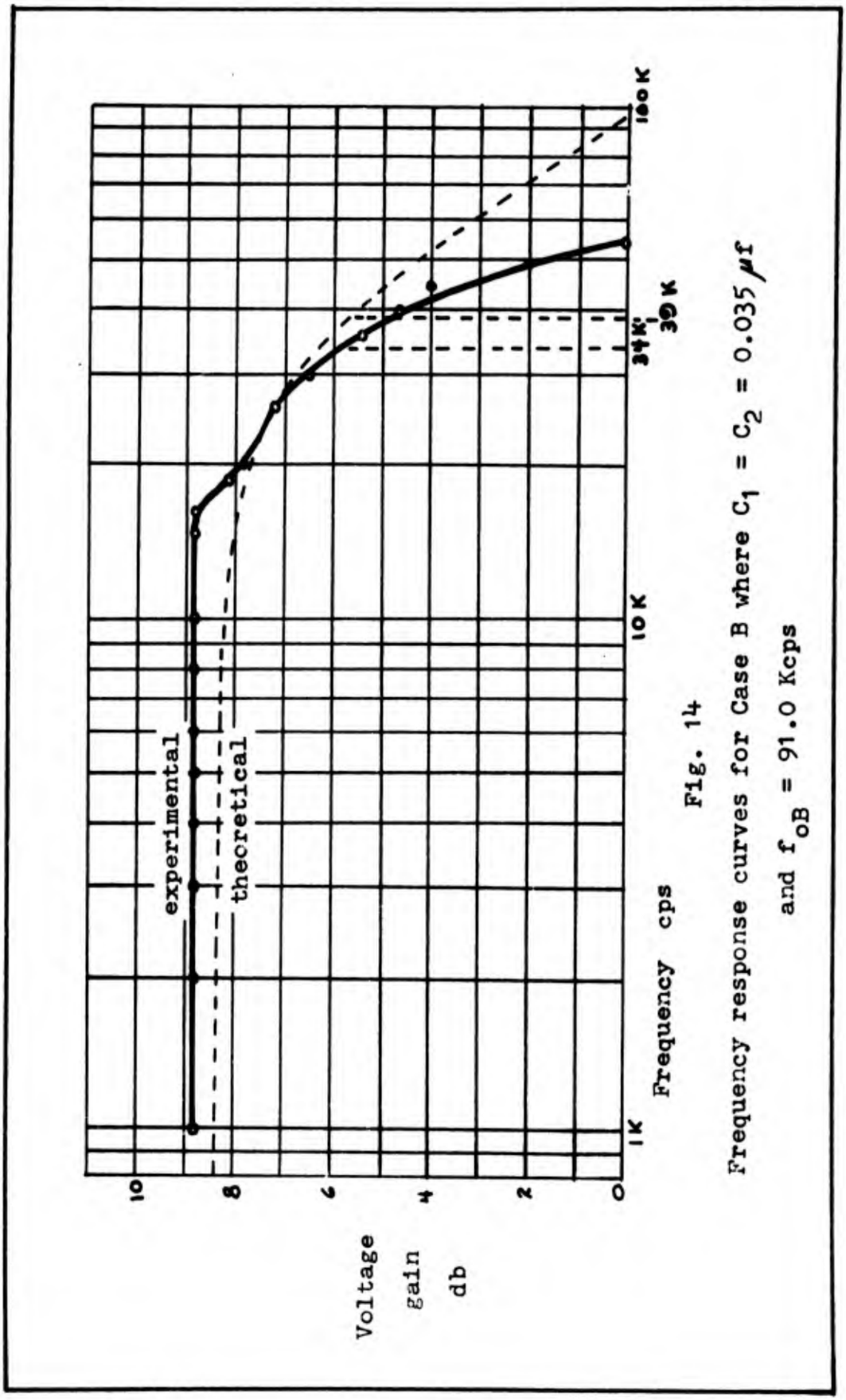

Fig. 14

Frequency response curves for Case B where $C_1 = C_2 = 0.035 \mu f$ and $f_{oB} = 91.0$ Kcps

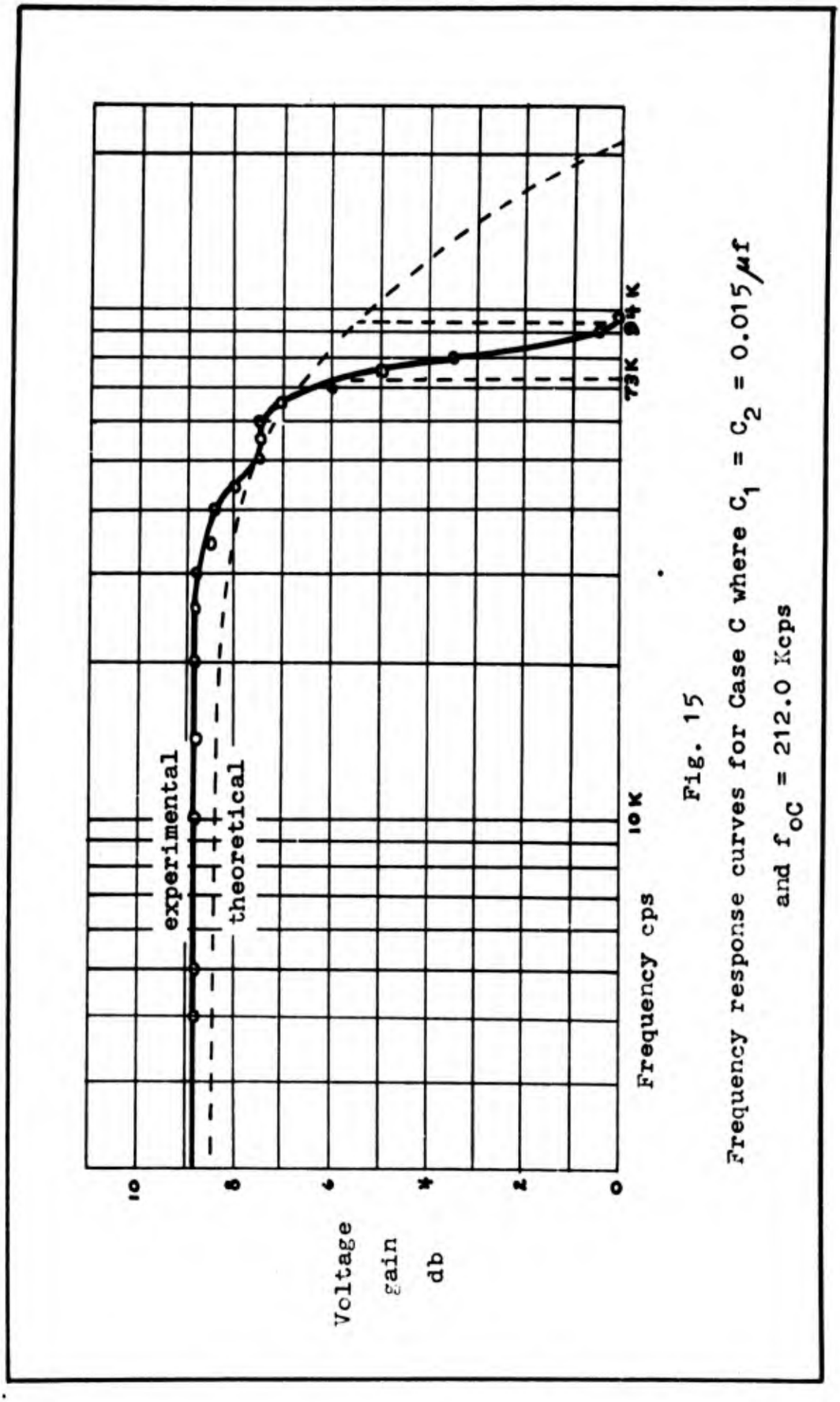

Fig. 15

Frequency response curves for Case C where $C_1 = C_2 = 0.015 \mu f$ and $f_{oC} = 212.0$ Kcps

cases. As a means of showing the comparison of the theoretical values and the measured values, the theoretical values are shown as dashed lines in the three figures.

The gain from the experimental curves in each case is approximately 8.80 db or a voltage gain of 2.75 which compares favorably with the theoretical maximum gain calculated for the circuit. Since the circuit was synthesized from Eq 29, the theoretical maximum voltage gain should be 2.67 or 8.54 db as previously calculated for f = 0 cps. The difference between 2.75 and 2.67 is within the experimental error. The cause of this difference is probably the method used to measure the input and the output signal voltages.

However, the bandwidth of the experimental circuit did not compare well with the theoretical bandwidth of the transfer function. At frequencies from 0 to 1000 cps there is no data because the input and output signal waveshapes were completely distorted. In this frequency range, one diode was removed, replaced, and then the other diode was removed to determine the cause of the distortion. This procedure showed that both diodes were oscillating. Because of the time limitation, the exact cause of this oscillation was not determined, but the probable cause is the poor isolation between the ac circuit and the dc biasing circuit. This would change the ac circuit completely because of the added inductance, capacitance, and resistance. Possibly the change

violated the ac stability criterion of Eq 5 where

$$R_T > \frac{L_T}{C\,|r_n|} \tag{39}$$

must be maintained for amplification. The poor isolation would also cause the Q-point of both tunnel diodes to change. This results in a change in the amount of negative resistance; consequently, the action of the circuit would not be that of the desired transfer function. One of these or all of these factors contribute to the unpredictable results in the frequency range from 0 to 1000 cps.

From 1000 cps to near the first corner frequency, the correlation between the theoretical and experimental values of voltage gain in each case are very good as mentioned earlier. In this frequency range, the circuit is extremely sensitive to a variation of Q-point for each of the tunnel diodes. Since the isolation between the ac signal and the dc biasing circuit was not perfect, the variable resistors in the bias circuit was used to maintain the same Q-point at each frequency that data (Appendix D) was taken.

As the first theoretical corner frequency was approached in each case, the actual response dropped off rapidly. This caused the bandwidth of the experimental circuit to be much smaller than in the theoretical case. In Case A, the difference in bandwidth between the experimental and the theoretical values is only 2.0 Kcps. As the capacitance in each

of the shunt branches (C_1 and C_2 of Fig. 11) was decreased, the corner frequencies increased. This is seen by comparing Figs. 13, 14, and 15. But when the corner frequencies were increased, the difference between the experimental and the theoretical bandwidth increased. From these results, it is concluded that the parasitic or stray capacitances in the circuit must be causing this poor high frequency response. This, in turn, causes the measured bandwidth of the amplifier to be less than the theoretical bandwidth.

V. Conclusions and Recommendations

The predistortion procedure for designing multistage tunnel diode amplifiers is a feasible solution to the cascading problem associated with the tunnel diode. An experimental amplifier containing two tunnel diodes has been designed, constructed, and evaluated as to gain, bandwidth, and complexity of the circuit. The gain and bandwidth were compared with the theoretical values obtained from the transfer function that was the basis for the synthesis of the circuit.

The close correlation between the actual gain and the theoretical gain was extremely good, but the bandwidths were not comparable. Below 1000 cps the tunnel diodes oscillated. Near the first theoretical corner frequency, the amplifier frequency response decreased sharply causing the bandwidth to be much less than the theoretical value.

The exact cause of the oscillation of the tunnel diodes was not determined, but the most probable cause is the poor isolation between the ac circuit and the dc biasing circuit at this low frequency. This causes the ac circuit to become somewhat different from the desired circuit which represents the original transfer function. Another effect of poor isolation is the change in Q-point of the tunnel diodes; thus, changing the negative resistance value from the necessary value. This, again, changes the circuit from the desired circuit.

The poor high frequency response near the first corner frequency was concluded to be partly caused by the effect of parasitic or stray capacitances. A solution of this problem would be more discriminate placement of components and better dressing of leads.

This report has proven the feasibility of the predistortion method. It has also uncovered some problems than should be investigated for the practical realization of a circuit synthesized by this method. These problems are design of a stable power supply for biasing the tunnel diode simply and achieving better isolation between the dc bias circuit and the ac signal circuit. These two problems along with the investigation of the cause of the erratic circuit operation below 1000 cps and further study of the reverse predistortion procedure are recommended for future studies.

Bibliography

1. Balabanian, N. Network Synthesis, Englewood Cliffs, N.J.: Prentice-Hall, Inc., 1958.

2. Gartner, W.W. "Esaki or Tunnel Diodes." Semiconductor Products, 3:36-38 (June 1960).

3. General Electric Company. Tunnel Diode Manual, (First Edition). Liverpool, N.Y.: The General Electric Co., 1961.

4. Gottlieb, E. "Using the Tunnel Diode." Electronic Industries, 19:110-113 (March 1960).

5. Hall, R.N. "Tunnel Diodes." IRE Transaction on Electron Devices, ED-7:1-9 (January 1960).

6. Kuh, E.S. and Pederson, D.O. Principles of Circuit Synthesis, N.Y.: McGraw-Hill Book Co., Inc., 1959.

7. Lesk, I.A. and Suran, J.J. "Tunnel Diode Operation and Application." Electrical Engineering, 79:270-277 (April 1960).

8. Roberts, G.N. "Tunnel Diodes-Operation and Application." Electronic Technology, 37:217-222 (June 1960).

9. Storer, J.E. Passive Network Synthesis, N.Y.: McGraw-Hill Book Co., Inc., 1957.

10. Sommers, H.S., Jr. "Tunnel Diodes as High Frequency Devices." Proceedings of the IRE, 47:1201-1206 (July 1959)

11. Van Der Ziel, A. Solid State Physical Electronics, Englewood Cliffs, N.J.: Prentice-Hall, Inc., 1957.

12. Van Valkenburg, M.E. Modern Network Synthesis, N.Y.: John Wiley and Sons, Inc., 1960.

13. Weinberg, L. "Synthesis Using Tunnel Diodes and Masers." IRE Transaction on Circuit Theory, CT-8:66-75 (March 1961)

Appendix A

Degenerate Semiconductor

The usual band picture for an n-type semiconductor is shown in Fig. A-1(a)(Ref 11:83-84). The donor impurity

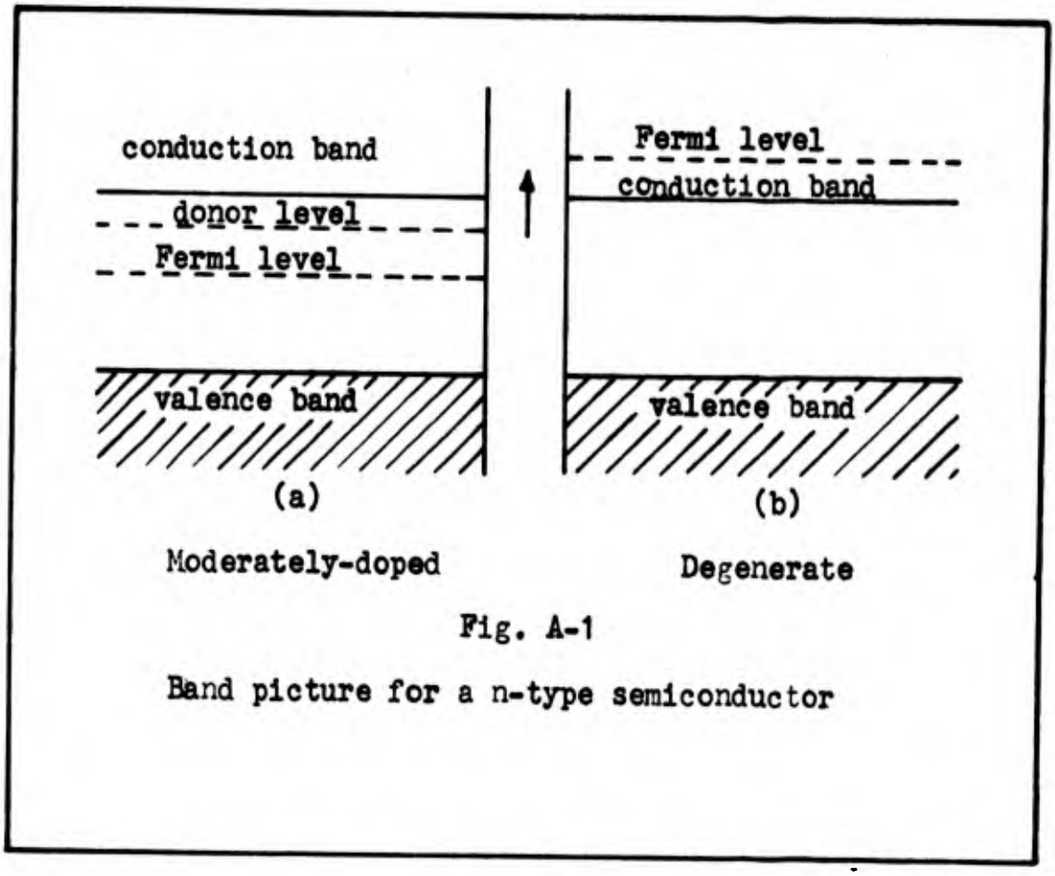

Fig. A-1

Band picture for a n-type semiconductor

level just below the bottom of the conduction band has the effect of an equal number of free electrons in the conduction band. Since the donor concentration is small, only a small fraction of the states in the conduction band are occupied; therefore, the Fermi Level is slightly above the middle of the forbidden band.

If the n-type semiconductor doping is increased more

and more until the impurity concentration becomes very large, around 10^{19} per cubic centimeter (Ref 7:270), all the states near the bottom of the conduction band will be occupied by electrons. This causes the Fermi Level to move up into the conduction band as shown in Fig. A-1(b). Such a material is called a degenerate n-type semiconductor.

Similarily, a p-type semiconductor with the band picture of Fig. A-2(a) (Ref 11:84) can be degenerately doped to have a energy diagram as shown in Fig. A-2(b).

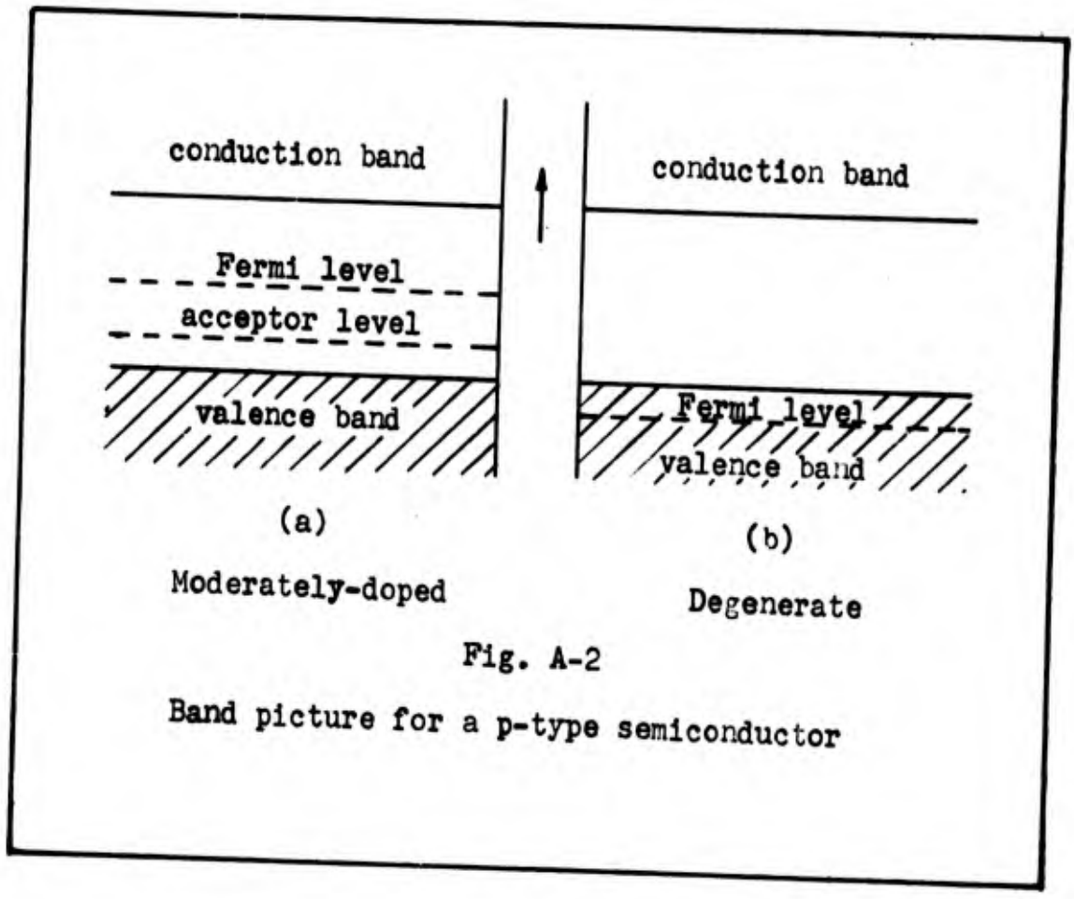

Fig. A-2

Band picture for a p-type semiconductor

Appendix B

Frequency Limits of the Tunnel Diode

The frequency limitations on the tunnel diode are due to the circuit parameters associated with the tunnel diode package. These four parameters are shown in the equivalent circuit of the tunnel diode in Fig. A-3. The frequency limits are the resistive cutoff frequency (f_{ro}), the maximum frequency that the amplifier can amplify, and the reactive cutoff frequency (f_{xo}), the frequency at which the reactive part of the diode impedance goes to zero.

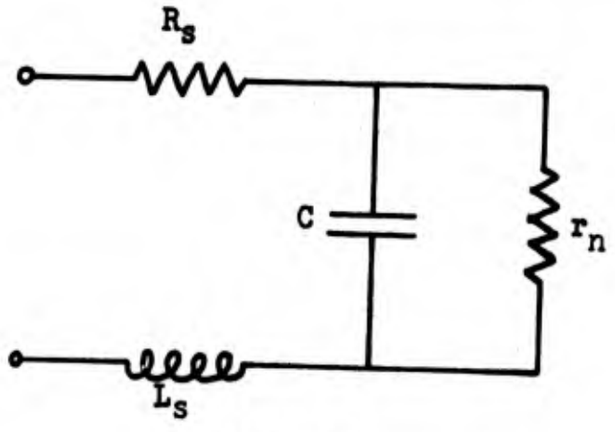

Fig. A-3

Equivalent circuit of the tunnel diode in the negative resistance region

The input impedance of the tunnel diode circuit is

$$Z_{in} = R_s + j\omega L_s + \frac{r_n\left(\frac{1}{j\omega C}\right)}{r_n + \frac{1}{j\omega C}} \qquad \text{(A-1)}$$

Simplifying

$$Z_{in} = R_s + j\omega L_s + \left(\frac{r_n}{1+j\omega r_n C}\right)\left(\frac{1-j\omega r_n C}{1-j\omega r_n C}\right)$$

$$= R_s + j\omega L_s + \frac{r_n - j\omega r_n^2 C}{1+\omega^2 r_n^2 C^2}$$

$$= \frac{R_s + \omega^2 r_n^2 C^2 R_s + r_n}{1+\omega^2 r_n^2 C^2} + \frac{j\omega L_s + j\omega^3 r_n^2 C^2 L_s - j\omega r_n^2 C}{1+\omega^2 r_n^2 C^2} \qquad \text{(A-2)}$$

To find the resistive cutoff frequency (f_{ro}), the real part of Eq A-2 is set equal to zero and solved for ω_{ro}. Since ω_{ro} is equal to $2\pi f_{ro}$, f_{ro} can easily be found.

$$R_s + \omega_{ro}^2 r_n^2 C^2 R_s + r_n = 0 \qquad \text{(A-3)}$$

$$\omega_{ro} = \left(\frac{-r_n - R_s}{r_n^2 C^2 R_s}\right)^{\frac{1}{2}} \qquad \text{(A-4)}$$

$$= \frac{1}{|r_n| C}\left(\frac{|r_n|}{R_s} - 1\right)^{\frac{1}{2}}$$

$$\therefore \quad f_{ro} = \frac{1}{2\pi C|r_n|}\left(\frac{|r_n|}{R_s} - 1\right)^{\frac{1}{2}} \qquad \text{(A-5)}$$

To find the reactive cutoff frequency (f_{xo}), the imaginary part of Eq A-2 is set equal to zero and solved for ω_{xo}. Since ω_{xo} is equal to $2\pi f_{xo}$, f_{xo} can easily be found as in the case for the resistive cutoff frequency.

$$L_s + \omega_{xo}^2 r_h^2 C^2 L_s - r_h^2 C = 0 \tag{A-6}$$

$$\omega_{xo} = \left(\frac{r_h^2 C - L_s}{r_h^2 C^2 L_s} \right)^{\frac{1}{2}} \tag{A-7}$$

$$= \left(\frac{1}{L_s C} - \frac{1}{r_h^2 C^2} \right)^{\frac{1}{2}}$$

$$\therefore \quad f_{xo} = \frac{1}{2\pi} \left(\frac{1}{L_s C} - \frac{1}{r_h^2 C^2} \right)^{\frac{1}{2}} \tag{A-8}$$

Appendix C

Synthesis of the Two Tunnel-Diode Amplifier

The amplifier used to demonstrate the use of the predistortion technique was designed by a method devised by E.S. Kuh (Ref 12:437-444). The model to which this method applies is shown in Fig. A-4. In this figure, it is assumed

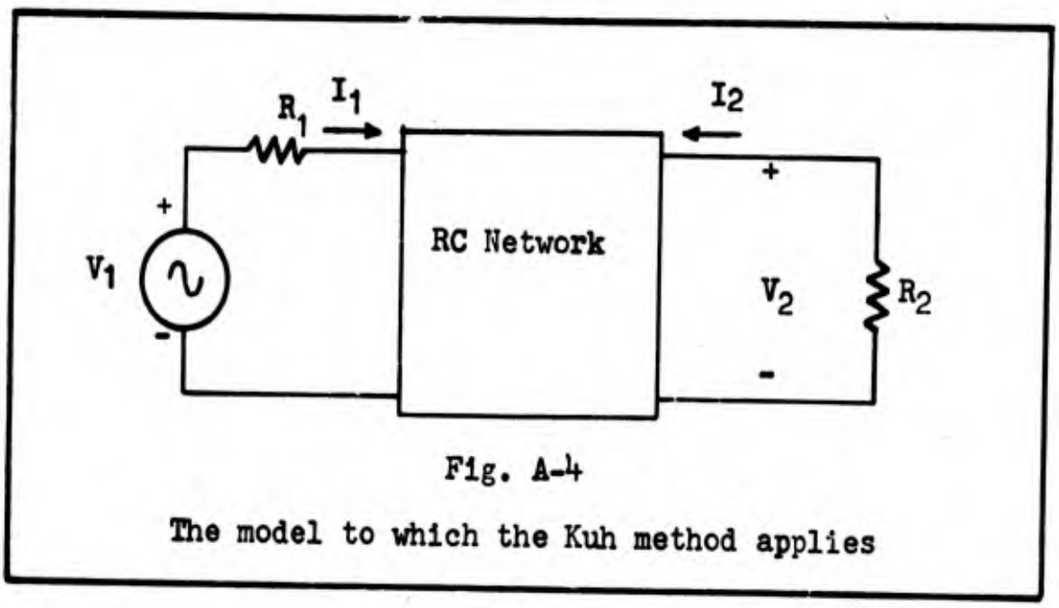

Fig. A-4

The model to which the Kuh method applies

that one of the input and one of the output terminals are connected together (grounded), the transfer function given is the forward voltage gain $G_{12} = V_2/V_1$, and the resistances R_1 and R_2 are known. In factored form G_{12} may be written

$$G_{12}(s) = K \frac{(s + a_1)(s + a_2) \ldots\ldots (s + a_i)}{(s + b_1)(s + b_2) \ldots\ldots (s + b_j)} \qquad \text{(A-9)}$$

where

$$j \geq i + 2$$

The normalized values specified as a basis for the amplifier synthesis are

$$G_{12}(s) = K \frac{1}{(s+\frac{1}{2})(s+\frac{3}{2})} \qquad (A\text{-}10)$$

$$R_1 = R_2 = 1$$

Amount of predistortion d = 1/2

When the predistortion is added, the predistorted transfer function is

$$G'_{12}(s) = K' \frac{1}{(s+1)(s+2)} \qquad (A\text{-}11)$$

The next step is to determine $-y_{12}$.

Since

$$G'_{12}(s) = \frac{V_2}{V_1} = \frac{-I_2 R_2}{V_1} = -y_{12} R_2 \qquad (A\text{-}12)$$

then

$$-y_{12} = \frac{G'_{12}}{R_2} = \frac{K'}{R_2}\left[\frac{1}{(s+1)(s+2)}\right] \qquad (A\text{-}13)$$

and the partial fraction expansion is

$$\frac{-y_{12}}{s} = \frac{K'}{R_2}\left[\frac{k_{12}^{(0)}}{s} + \frac{k_{12}^{(1)}}{s+1} + \frac{k_{12}^{(2)}}{s+2}\right]$$

$$= \frac{K'}{1}\left[\frac{\frac{1}{2}}{s} + \frac{-1}{s+1} + \frac{\frac{1}{2}}{s+2}\right] \qquad (A\text{-}14)$$

From this equation y_{11} and y_{22} may be selected to satisfy the residue condition

$$k_{11}^{(i)}\, k_{22}^{(i)} = \left[k_{12}^{(i)}\right]^2 \qquad (A\text{-}15)$$

Therefore,

$$\frac{y_{11}}{s} = K'\left(\frac{\frac{1}{2}}{s} + \frac{x_1}{s+1} + \frac{x_2}{s+2}\right) \qquad \text{(A-16)}$$

and

$$\frac{y_{22}}{s} = K'\left(\frac{\frac{1}{2}}{s} + \frac{\frac{1}{x_1}}{s+1} + \frac{\frac{1}{4x_2}}{s+2}\right) \qquad \text{(A-17)}$$

At infinite frequency, $y_{11} = \frac{1}{R_1} = 1$ and $y_{22} = \frac{1}{R_2} = 1$, so that from Eqs A-16 and A-17

$$K'\left(\tfrac{1}{2} + x_1 + x_2\right) = 1 \qquad \text{(A-18)}$$

and

$$K'\left(\tfrac{1}{2} + \frac{1}{x_1} + \frac{1}{4x_2}\right) = 1 \qquad \text{(A-19)}$$

From Eqs A-18 and A-19, x_1 and x_2 must be solved in such a way that K' is a maximum. From the Kuh method

$$\frac{x_1}{\left|k_{12}^{(1)}\right|} = \frac{x_2}{\left|k_{12}^{(2)}\right|} = X \qquad \text{(A-20)}$$

where X must satisfy the quadratic equation

$$X^2 + \frac{k_{12}^{(0)}}{A}\left(1 - \frac{R_2}{R_1}\right)X - \frac{R_2}{R_1} = 0 \qquad \text{(A-21)}$$

where

$$A = \sum_{i=1}^{m} \left|k_{12}^{(i)}\right| \qquad \text{(A-22)}$$

Then the maximum value of K' is

$$K'_{max} = \frac{R_2/R_1}{k_{12}^{(0)} + XA} \qquad \text{(A-23)}$$

and y_{11}, $-y_{12}$, and y_{22} are determined.

Applying Eqs A-20,21,22, and 23 to the synthesis problem,

$$x_1 = 2x_2 = X \tag{A-24}$$

and Eq A-21 becomes

$$X^2 - 1 = 0$$

$$X = 1$$

Therefore, $x_1 = 1$ and $x_2 = 1/2$ making $K' = 1/2$.

Then from Eq A-16

$$\frac{y_{11}}{s} = \frac{1}{2}\left(\frac{\frac{1}{2}}{s} + \frac{1}{s+1} + \frac{\frac{1}{2}}{s+2}\right)$$

$$y_{11} = \frac{2s^2 + 4s + 1}{2s^3 + 6s + 4} \tag{A-25}$$

The continued fraction expansion of y_{11} is

$$\begin{array}{r|l}
2s^2+4s+1 & 1 \\
\hline
2s+3 & 2s^2+4s+1 \;\big|\; s \\
\hline
s+1 & 2s^2+3s \;\big|\; 2 \\
\hline
1 & 2s+2 \;\big|\; s \\
\hline
1 & s \;\big|\; 1 \\
\hline
 & 1 \\
\hline
 & 0
\end{array} \tag{A-26}$$

Appendix D

Experimental Data For Frequency Response Curves

Table II

Experimental Data For The Frequency Response Curve For Case A

$C_1 = C_2 = 0.055$ microfarads

$E_{in} = 28.3$ millivolts

Frequency (Kcps)	E_{out} (mv)	$_vG_f$ (ratio)	vG_f (db)
1.0	78.0	2.75	8.80
2.0	78.0	2.75	8.80
4.0	78.0	2.75	8.80
6.0	78.0	2.75	8.80
8.0	78.0	2.75	8.80
10.0	78.0	2.75	8.80
12.0	74.4	2.63	8.40
14.0	70.8	2.50	7.96
16.0	69.3	2.45	7.78
18.0	67.2	2.38	7.52
20.0	63.7	2.25	7.06
22.0	60.2	2.13	6.56
24.0	56.6	2.00	6.00
26.0	49.6	1.75	4.86
28.0	42.5	1.50	3.52
30.0	39.6	1.40	2.92
32.0	38.2	1.35	2.60
34.0	36.8	1.30	2.28
36.0	35.4	1.25	1.94
40.0	28.3	1.00	0.00

Table III

Experimental Data For The Frequency Response Curve For Case B

$C_1 = C_2 = 0.035$ microfarads

$E_{in} = 28.3$ millivolts

Frequency (Kcps)	E_{out} (mv)	$_vG_f$ (ratio)	$_vG_f$ (db)
1.0	78.0	2.75	8.80
2.0	78.0	2.75	8.80
3.0	78.0	2.75	8.80
4.0	78.0	2.75	8.80
5.0	78.0	2.75	8.80
6.0	78.0	2.75	8.80
8.0	78.0	2.75	8.80
10.0	78.0	2.75	8.80
15.0	78.0	2.75	8.80
16.0	78.0	2.75	8.80
18.0	73.0	2.58	8.20
20.0	70.0	2.48	7.88
26.0	64.5	2.28	7.14
30.0	60.2	2.13	6.54
36.0	52.4	1.85	5.34
40.0	49.6	1.73	4.74
45.0	45.3	1.60	4.08
50.0	35.4	1.25	1.94
55.0	28.3	1.00	0.00

Table IV

Experimental Data For The Frequency Response Curve For Case C

$C_1 = C_2 = 0.015$ microfarads

$E_{in} = 28.3$ millivolts

Frequency (Kcps)	E_{out} (mv)	$_vG_f$ (ratio)	$_vG_f$ (db)
1.0	78.0	2.75	8.80
2.0	78.0	2.75	8.80
3.0	78.0	2.75	8.80
4.0	78.0	2.75	8.80
5.0	78.0	2.75	8.80
10.0	78.0	2.75	8.80
15.0	78.0	2.75	8.80
20.0	78.0	2.75	8.80
25.0	78.0	2.75	8.80
30.0	78.0	2.75	8.80
35.0	74.4	2.63	8.40
40.0	74.4	2.63	8.40
45.0	70.8	2.50	7.96
50.0	67.2	2.38	7.52
55.0	67.2	2.38	7.52
60.0	67.2	2.38	7.52
65.0	63.7	2.25	7.06
70.0	56.6	2.00	6.00
75.0	49.6	1.75	4.86
80.0	42.5	1.50	3.52
85.0	35.4	1.25	1.94
90.0	28.7	1.05	0.42
95.0	28.3	1.00	0.00

Vita

Richard R. Wong was born [redacted], the son of Kee Brown Wong and Jue Shee Brown Wong. After completing his work in 1949 at [redacted], he enrolled at Oregon State College, Corvallis, Oregon. In June 1953 he was graduated with the degree of Bachelor of Science in Electrical Engineering. After receiving his commission as a Lieutenant in the USAF Reserves, he entered active duty in November 1953. He attended the Airborne Electronics Officers ccurse at Keesler AFB, Mississippi. Upon completion of the course, he was sent to Laon AFB, France. His military assignment prior to his coming to the Air Force Institute of Technology was instructor in basic electronics at Mather AFB, California.

Permanent address: [redacted]

This thesis was typed by Mrs. Kathleen Purple and the author.

UNCLASSIFIED